Measuring Molecular Order in Poly(3-alkylthiophene) Thin Films with Polarizing Spectroscopies

Marc C. Gurau,[†] Dean M. Delongchamp,[‡] Brandon M. Vogel,[‡] Eric K. Lin,[‡] Daniel A. Fischer,[§] Sharadha Sambasivan,[§] and Lee J. Richter*,[†]

Surface and Microanalysis Science Division, Chemical Science and Technology Laboratory, Polymers Division, Materials Science and Engineering Laboratory, and Ceramics Division, Materials Science and Engineering Laboratory, National Institute of Standards and Technology, 100 Bureau Drive, Mail Stop 8372, Gaithersburg, Maryland 20899

Received June 30, 2006. In Final Form: October 5, 2006

We measured the molecular order of poly(3-alkylthiophene) chains in thin films before and after melting through the combination of several polarized photon spectroscopies: infrared (IR) absorption, variable angle spectroscopic ellipsometry (SE), and near-edge X-ray absorption fine structure (NEXAFS). The data from the various techniques can be uniformly treated in the context of the dielectric constant tensor ϵ for the film. The combined spectroscopies allow determination of the orientation distribution of the main-chain axis (SE and IR), the conjugated π system normal (NEXAFS), and the side-chain axis (IR). We find significant improvement in the backbone order of the films after recrystallization of the material at temperatures just below the melting temperature. Less aggressive thermal treatments are less effective. IR studies show that the changes in backbone structure occur without significant alteration of the structure of the alkyl side chains. The data indicate that the side chains exhibit significant disorder for all films regardless of the thermal history of the sample.

Introduction

Interest in organic semiconductors has increased significantly because of their potential use in low cost, high volume electronics applications such as radio frequency identification tags, biosensors, or photovoltaics. The development of solution processable organic semiconductors has made it possible to take advantage of fabrication methods such as spin coating, dip coating, or ink-jet printing onto flexible substrates.[1] Of the early solution processable polymers, semiconducting poly(3-alkylthiophenes) (P3ATs) provide relatively high field effect mobilities and have been employed as *p*-type semiconductors in organic field effect transistors (OFETs) and photovoltaic devices. Reports establish that there exists substantial variability in the device performance that can be achieved with P3AT films.[2−12] Some of the observed variability has been attributed to the development of different film morphologies.[5,8,9] Studies on spin cast P3AT thin films have shown that changes in field effect mobility correlate to changes in the alkyl side-chain length,[2] polymer molecular weight,[9,10] solvent,[11] casting method,[13] and the thermal history of the sample.[10]

The regioregular P3ATs are nominally semicrystalline, rigid-rod polymers that are thought to adopt a π stacked, lamellar structure in ordered regions. In early grazing X-ray diffraction studies of poly(3-hexylthiophene) P3HT films, it was found that mobility strongly correlated with molecular orientation. Face-on orientation, where the conjugated backbone lays parallel to the substrate surface, gives rise to lower mobilities than edge-on orientation.[14] For consistently edge-on orientations, higher mobilities were correlated with greater regioregularity via the development of improved π stacking, evidenced by the development of an interchain exciton−polaron at 2.03 eV.[14,15] The critical structural motif for charge transport has been questioned in recent studies of the molecular weight dependence of the performance of P3HT. Low molecular weight (MW) material has an extremely high crystalline order, forming ribbon-like nanocrystals. However, its mobility is significantly lower than that of high MW material, with small, poorly ordered domains. This observation has led to proposals that either grain boundary effects[9] or conjugation length effects[10] play a dominant role. The problem of optimizing the material parameters of P3ATs is complicated by the realization that the films are rarely in an equilibrium structure. Variations in performance with deposition method (spin vs cast) and conditions (solvent, spin speed) have been reported.[7,11,13,14] In

* Corresponding author. E-mail: lee.richter@nist.gov. Phone: (301) 975-4152.

[†] Surface and Microanalysis Science Division.

[‡] Polymers Division.

[§] Ceramics Division.

(1) Gamota, D. R. *Printed organic and molecular electronics*; Kluwer Academic: Boston, 2003.

(2) Babel, A.; Jenekhe, S. A. *Synth. Met.* **2005**, *148* (2), 169−173.

(3) Raja, M.; Lloyd, G. C. R.; Sedghi, N.; Eccleston, W.; Di Lucrezia, R.; Higgins, S. J. *J. Appl. Phys.* **2002**, *92* (3), 1441−1445.

(4) Sirringhaus, H.; Tessler, N.; Friend, R. H. *Science* **1998**, *280* (5370), 1741−1744.

(5) Sirringhaus, H.; Brown, P. J.; Friend, R. H.; Nielsen, M. M.; Bechgaard, K.; Langeveld-Voss, B. M. W.; Spiering, A. J. H.; Janssen, R. A. J.; Meijer, E. W. *Synth. Met.* **2000**, *111*, 129−132.

(6) Chua, L. L.; Zaumseil, J.; Chang, J. F.; Ou, E. C. W.; Ho, P. K. H.; Sirringhaus, H.; Friend, R. H. *Nature (London)* **2005**, *434* (7030), 194−199.

(7) Bao, Z.; Dodabalapur, A.; Lovinger, A. J. *Appl. Phys. Lett.* **1996**, *69* (26), 4108−4110.

(8) Kim, D. H.; Park, Y. D.; Jang, Y. S.; Yang, H. C.; Kim, Y. H.; Han, J. I.; Moon, D. G.; Park, S. J.; Chang, T. Y.; Chang, C. W.; Joo, M. K.; Ryu, C. Y.; Cho, K. W. *Adv. Funct. Mater.* **2005**, *15* (1), 77−82.

(9) Kline, R. J.; McGehee, M. D.; Kadnikova, E. N.; Liu, J. S.; Frechet, J. M. J.; Toney, M. F. *Macromolecules* **2005**, *38* (8), 3312−3319.

(10) Zen, A.; Pflaum, J.; Hirschmann, S.; Zhuang, W.; Jaiser, F.; Asawapirom, U.; Rabe, J. P.; Scherf, U.; Neher, D. *Adv. Funct. Mater.* **2004**, *14* (8), 757−764.

(11) Chang, J. F.; Sun, B. Q.; Breiby, D. W.; Nielsen, M. M.; Solling, T. I.; Giles, M.; McCulloch, I.; Sirringhaus, H. *Chem. Mater.* **2004**, *16* (23), 4772−4776.

(12) Goh, C.; Kline, R. J.; McGehee, M. D.; Kadnikova, E. N.; Frechet, J. M. J. *Appl. Phys. Lett.* **2005**, *86* (12).

(13) DeLongchamp, D. M.; Vogel, B. M.; Jung, Y.; Gurau, M. C.; Richter, C. A.; Kirillov, O. A.; Obrzut, J.; Fischer, D. A.; Sambasivan, S.; Richter, L. J.; Lin, E. K. *Chem. Mater.* **2005**, *17* (23), 5610.

(14) Sirringhaus, H.; Brown, P. J.; Friend, R. H.; Nielsen, M. M.; Bechgaard, K.; Langeveld-Voss, B. M. W.; Spiering, A. J. H.; Janssen, R. A. J.; Meijer, E. W.; Herwig, P.; de Leeuw, D. M. *Nature (London)* **1999**, *401* (6754), 685−688.

(15) Brown, P. J.; Thomas, D. S.; Kohler, A.; Wilson, J. S.; Kim, J. S.; Ramsdale, C. M.; Sirringhaus, H.; Friend, R. H. *Phys. Rev. B* **2003**, *67* (6).

10.1021/la0618972 CCC: $37.00
Published on Web 12/19/2006

this paper, we show that the structural evolution of P3AT spin cast films can be determined as a function of thermal treatment with several polarized optical spectroscopies. Near edge X-ray absorption fine structure (NEXAFS) spectroscopy, transmission ultraviolet−visible (UV−vis) spectroscopy, and variable-angle spectroscopic ellipsometry (SE) were used to characterize the ordering of the conjugated backbone. Infrared absorption spectroscopy (IR) provided further information about backbone ordering and direct insights into the relationship between backbone and side-chain order. Importantly, these methods probe the entirety of the thin film, both crystalline and noncrystalline regions.

Experimental Procedures

Substrate Preparation and Film Fabrication. Films were spin coated onto either double side polished *p*-type ⟨100⟩ Si wafers or fused quartz plates. After a 5 min exposure to an oxygen plasma, Si wafers were stripped of their native oxide in a buffered oxide etch for 3 min. Following etching, an oxide layer was regrown by treatment in UV ozone for 10 min per side. The quartz plates were cleaned in a H_2O_2/H_2SO_4 (30%:70%) solution before being subjected to the same UV ozone treatment. After ozone treatment, both substrates presented hydrophilic oxide surfaces with water contact angles $\leq 6°$. These substrates were then rendered hydrophobic by a 5 min vapor deposition of hexamethyldisilazane (HMDS) in a vacuum oven at 120 °C. This exposure created a submonolayer coverage of methyl groups on the oxide surface and resulted in water contact angles near 50°.

Regioregular, head-to-tail P3HT (HT-P3HT) samples were obtained from Plextronics (Plextronics Inc., Pittsburgh, PA),[16] while regiorandom P3HT (R-P3HT) and regioregular poly(3-octylthiophene) (HT-P3OT) samples were obtained from Aldrich.[16] All polymers were used as received. The vendor reported that the average MW of the three polymers was R-P3HT 300 kDa, HT-P3HT 18 kDa, and HT-P3OT 50 kDa. As-cast films were cast by spin coating from 2 mg/mL chloroform solutions at 209 rad/s (2000 rpm). All solutions were passed through a 0.45 μm PTFE filter. As-cast films were placed in a dark N_2 purge box until analysis. Thermally treated films were placed into a vacuum [(10^{-2} to 10^{-3}) Pa and (10^{-4} to 10^{-5}) Torr] environment and heated above their melting temperature for 1 h (250 °C for all films) before the films were allowed to crystallize (180 °C for HT-P3HT[17] and 150 °C for R-P3HT[17] and HT-P3OT[17]) at temperatures just below their melting temperature overnight. The resulting films ranged from 25 nm to 32 nm in thickness as measured by SE. All films were stored in a dark, nitrogen environment between measurements. No birefringence was observed in polarizing microscopy, suggesting that the grain size of any crystallites was small.

NEXAFS. NEXAFS spectroscopy was performed at the NIST/Dow soft X-ray materials characterization facility (beamline U7A) at the National Synchrotron Light Source (NSLS) of Brookhaven National Laboratory. Orientation was characterized by collecting carbon K-edge spectra in partial electron yield (PEY) mode with a grid bias of −50 V, corresponding to a surface-weighted sampling depth of ≈6 nm. The experimental standard uncertainty in the peak position for PEY spectra was ±0.15 eV; the yield uncertainty was ±2%. Incident angles Θ (with respect to the surface plane) were varied at seven angles between 20° and 70°. The $1s \rightarrow \pi^*$ resonance intensity was determined by fitting a Voigt function to the peak near 285 eV and dividing the peak area by the signal intensity at 330 eV, which is an orientation insensitive measure of the carbon atom density within the sampling volume. The intensities, thus normalized, were then fit to $\sin^2 \Theta$. This linear fit was used to extrapolate intensities at 0 and 90° incidence, which were then used to calculate the figure-of-merit $R = (I(90) - I(0))/(I(90) + I(0))$. For a system with the conjugated plane face-on to the surface $R = -1$. Because of nonidealities in the polarization state of the beam, a system with the conjugated plane purely edge-on would exhibit an $R \approx 0.7$.

Ellipsometry and Transmission UV−Vis. Ellipsometric data at multiple angles (45°, 27.5°, and 10° with respect to the surface plane) from polymer films spun on double side polished Si wafers was obtained with an M-2000 series spectroscopic ellipsometer (J. A. Woollam Co., Inc., Lincoln, Ne).[16] Unique determination of the uniaxial dielectric function from films as thin as used here is problematic based only on SE data. (Throughout this paper, the term dielectric function will refer to the unitless, relative dielectric function, ϵ_r, and the subscript r will be omitted. The real and imaginary parts of ϵ are denoted by primes: $\epsilon = \epsilon' + i\epsilon''$.) Therefore, normal incidence transmission UV−vis spectra were acquired from films spun onto transparent quartz substrates using a Lambda 2 spectrometer (Perkin-Elmer, Wellesley, MA). Both data sets were then fit simultaneously to a uniaxial model using vendor supplied analysis software. The dichroism exhibited by films in the visible region was quantified as the ratio of the imaginary parts of the out-of-plane and in-plane dielectric functions: $\epsilon''_z/\epsilon''_{x,y}$. The SE data were additionally augmented by limited IR ellipsometry data in the range of 8000−500 cm^{-1} recorded with a J. A. Woollam Co. IR-VASE.

Brewster's Angle Transmission FTIR. P3AT films on double side polished Si wafers were also investigated with polarized, Fourier transform IR (FTIR) spectroscopy. The sample compartment of a Magna 860 FTIR (Thermo Nicolet, Waltham, MA) was equipped with a simple transmission stage consisting of a variable angle goniometer used to position the sample at Brewster's angle ($\Theta \approx 16.3°$) with respect to the incident IR beam. The polarization of the infrared light was controlled by a wire grid polarizer placed immediately before the sample stage.

The transmitted spectra are reported as absorbance (base 10) by normalization to the spectra of blank wafers having undergone identical surface treatments. Each spectrum represents the average of 256 scans with a DTGS detector. All spectra were treated so as to remove peaks from atmospheric water and were baseline corrected. Additionally, a series of Fourier filters was applied to remove high frequency Etalon fringes that resulted from the IR transmission through the parallel Si substrates.

The infrared spectra were fit with a least squares regression of both *s*- and *p*-polarized spectra simultaneously. Data were fit to a sum of Lorentzian peaks whose positions (ω) and widths (Γ) were constrained to be the same for both polarizations, while the amplitudes (A) were allowed to vary independently. The dichroism exhibited by specific vibrational features is expressed as the ratio A_p/A_s of the Lorentzian peak amplitudes in the *p*- and *s*-polarized spectra.

Results

Visible and UV Spectroscopy. Figure 1 shows the optical transmission spectra of P3AT films spun onto HMDS treated quartz plates. UV−vis absorption is one of the most commonly applied techniques for semiconducting film characterization, and the as-cast data presented here are consistent with most reports.[2,9,10,18−20] The absorption maximum, λ_0, of R-P3HT in $CHCl_3$ solution appears near 428 nm. The peak slightly red-shifts to 450 nm in R-P3HT as-cast films, indicating almost no increase in conjugation length. It is accepted that the random alkyl-chain regiochemistry causes twists in the ring plane and severely limits the conjugation length. The solution λ_0 for HT-P3HT and HT-P3OT is 457 nm and 451 nm, respectively, and shifts to about 550 nm for films prepared from HT-P3HT and HT-P3OT. These shifts are consistent with a significant increase

(16) Certain commercial equipment, instruments, or materials are identified in this paper to foster understanding. Such identification does not imply recommendation or endorsement by the National Institute of Standards and Technology, nor does it imply that the materials or equipment identified are necessarily the best available for this purpose.

(17) Pal, S.; Nandi, A. K. *Macromolecules* **2003**, *36* (22), 8426−8432.

(18) Trznadel, M.; Pron, A.; Zagorska, M. *Macromolecules* **1998**, *31* (15), 5051−5058.

(19) Takashima, W.; Pandey, S. S.; Endo, T.; Rikukawa, M.; Tanigaki, N.; Yoshida, Y.; Yase, K.; Kaneto, K. *Thin Solid Films* **2001**, *393* (1−2), 334−342.

(20) Fell, H. J.; Samuelsen, E. J.; Alsnielsen, J.; Grubel, G.; Mardalen, J. *Solid State Commun.* **1995**, *94* (10), 843−846.

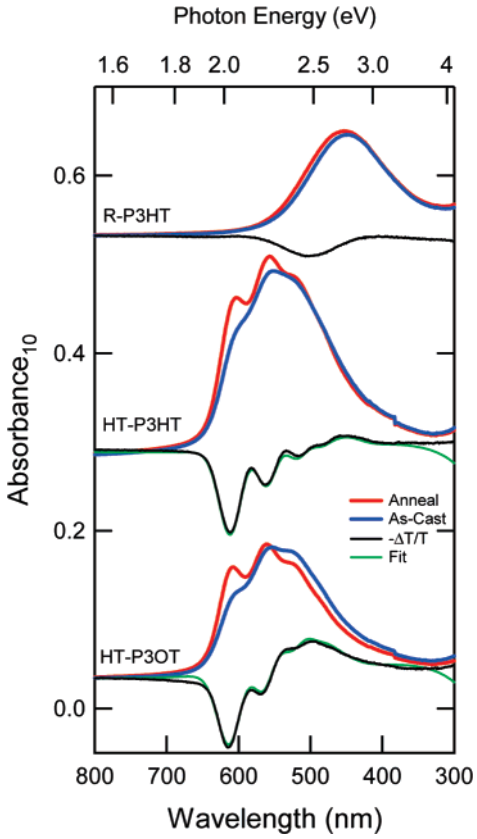

Figure 1. UV−vis absorbance (base 10) spectra of films of R-P3HT, HT-P3HT, and HT-P3OT on HMDS treated fused quartz plates before (blue) and after (red) thermal treatment (1 h at 250 °C followed by an overnight anneal at 150, 180, and 150 °C for R-P3HT, HT-P3HT, and HT-P3OT, respectively). The black lines are the normalized changes in the spectra upon heating. Green lines are fits to a Franck−Condon series as described in the text. Data from the different polymers have been offset for clarity.

Table 1. Franck−Condon Fitting Parameters Obtained from Fitting Thermally Induced Changes in Transmission Spectra

	HT-P3HT	HT-P3OT
E_0-0	2.03	2.02
S	0.86	0.95
ν_0	0.18	0.17

in conjugation length. In addition, there is a weak fine structure apparent in the absorption of the HT films. This absorption structure is consistent with a Franck−Condon coupled exciton−polaron series, again suggestive of improved film order.[15] The R-P3HT sample shows almost no change upon recrystallization, while HT-P3HT and HT-P3OT clearly exhibit improved resolution of the fine structure. Except for slight changes in the absolute intensity of the main optical absorption of HT-P3OT upon heating at elevated temperatures, the UV−vis data from HT-P3OT and HT-P3HT are very similar. These slight changes in intensity could result from small changes in film thickness because these spectra were recorded from two different films. The normalized difference in transmission intensity ($\Delta T/T$), also shown in Figure 1, shows a clear progression of evenly spaced features for both HT polymers. The ($\Delta T/T$) data can be well-fit by a single Franck−Condon series[21] and a slowly varying background to account for small changes in the broad primary absorption. The 0−0 transition energy, Huang−Rhys parameter S, and phonon mode frequency ν_0 are given in Table 1. The results are similar to those reported

(21) Pope, M.; Swenberg, C. E. *Electronic processes in organic crystals;* Clarendon Press: New York, 1982.

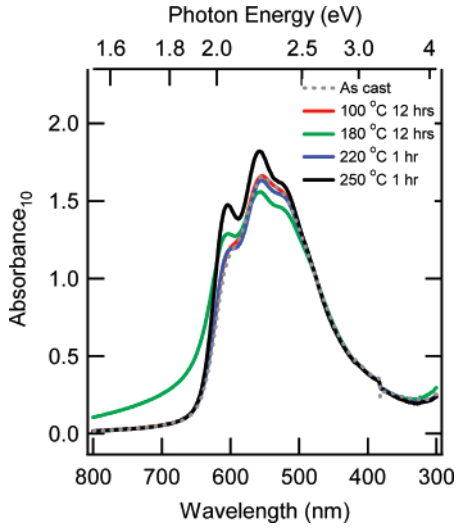

Figure 2. UV−vis absorbance (base 10) spectra of HT-P3HT films after different thermal treatments: 100 °C overnight, 180 °C overnight, 220 °C for 1 h, and 250 °C for 1 h. All spectra were normalized according to intensity at 475 nm.

by Brown et al.[22] based on fitting the charge modulation spectra of HT-P3HT and Sakuri et al.[23] based on fits to the UV−vis of HT-P3OT.

Shown in Figure 2 are UV−vis spectra for HT-P3HT recorded at room temperature after different thermal histories: as-cast, at 100 °C overnight, at 180 °C overnight, at 220 °C for 1 h, and at 250 °C for 1 h. All were performed in a nitrogen environment and followed by a slow cooling to room temperature. It is common in the literature to heat films to 60−100 °C to remove any residual solvent.[2,9,11,15] It is clear that this treatment negligibly alters the electronic spectrum. While heating the films at higher temperatures clearly alters the film order, further experiments with films heated to 250 °C and exposed to different cooling rates indicate that both heating above the melting temperature (250 °C) and recrystallization at a high temperature (180 °C) are needed to achieve the full change displayed in Figure 1, consistent with previously reported X-ray measurements.[24]

Further details about the film structure can be obtained from the uniaxial dielectric function extracted from the simultaneous analysis of the transmission and SE data. The imaginary part of the dielectric function, $\epsilon''_{x,y}$ (in-plane) and ϵ''_z (out-of-plane), from films spun on HMDS treated surfaces before and after recrystallization are shown in Figure 3. The majority of the optical absorption from all polymer samples lay within the plane of the film. The dichroism values ($\epsilon''_z/\epsilon''_{x,y}$) observed for these films at 2.25 eV are reported in Table 2. The values at 2.25 eV sample the nominal peak of the HT-P3HT and HT-P3OT absorptions and the red edge of the R-P3HT spectrum. The transition dipole moment for this $\pi-\pi^*$ transition lies along the chain axis.[25] The dichroism indicates the expected in-plane orientation of the chain axis ($\epsilon''_z/\epsilon''_{x,y} \ll 1$, see Disscussion). The regiorandom polymer exhibits a tendency toward less in-plane order (a higher $\epsilon''_z/\epsilon''_{x,y}$ ratio), but the order does improve slightly upon heating. The high degree of chain axis order of the regioregular material shows little change upon heating at higher temperatures.

(22) Brown, P. J.; Sirringhaus, H.; Harrison, M.; Shkunov, M.; Friend, R. H. *Phys. Rev. B* **2001**, *63* (12).

(23) Sakurai, K.; Tachibana, H.; Shiga, N.; Terakura, C.; Matsumoto, M.; Tokura, Y. *Phys. Rev. B* **1997**, *56* (15), 9552−9556.

(24) Hugger, S.; Thomann, R.; Heinzel, T.; Thurn-Albrecht, T. *Colloid Polym. Sci.* **2004**, *282* (8), 932−938.

(25) Erb, T.; Raleva, S.; Zhokhavets, U.; Gobsch, G.; Stuhn, B.; Spode, M.; Ambacher, O. *Thin Solid Films* **2004**, *450* (1), 97−100.

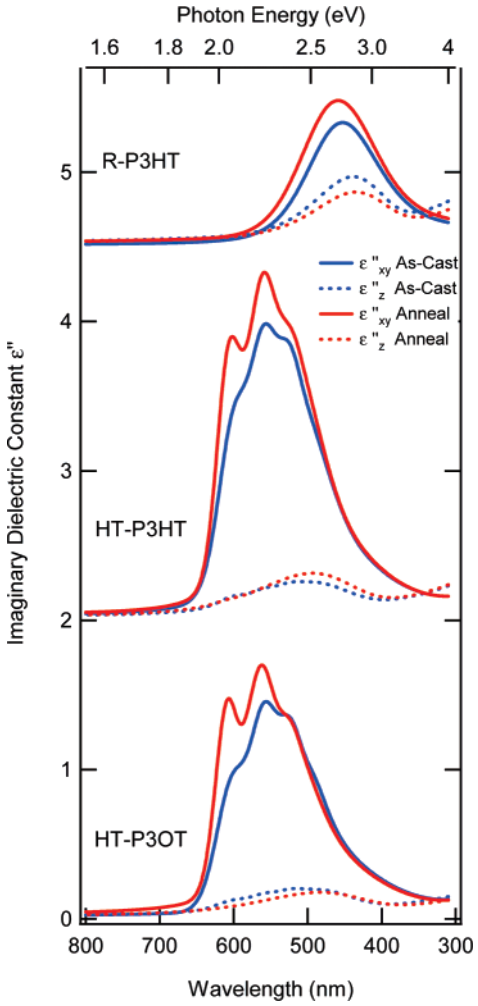

Figure 3. Uniaxial optical constants from simultaneous fits of both ellipsometric and transmission UV−vis data. In-plane ($k_{x,y}$) and out-of-plane (k_z) components of the model dielectric function are shown for high MW HT-P3HT spun onto HMDS treated oxide surfaces before (blue) and after (red) recrystallization. Data from the different polymers have been offset for clarity.

Despite its utility when applied to films of interest to the organic electronics community, spectroscopic ellipsometry has not been extensively applied to the characterization of the polyalkylthiophenes. In early studies, performed on P3HT films spun cast on Au from $CHCl_3$,[26−28] the degree of regioregularity of the polymer was not specified, and an isotropic model was used in the analysis, precluding assessment of the film anisotropy. However, the extracted absorption coefficient is similar to that found for our as-cast films. A critical point analysis identified three transitions at 2.05, 2.23, and 2.47 eV. The films were found to degrade on a time scale of days upon exposure to lab ambient conditions, characterized by a systematic blue-shift in the absorption spectrum. Recently, as-cast P3OT films have been characterized as a function of both spin speed and solvent.[29−31] The level of exciton−polaron structure in the reported ϵ'' spectra is less than but comparable to the as-cast films in this paper. The film anisotropy, as judged from $\epsilon''_z/\epsilon''_{x,y}$, varied from ≈0.25 to ≈0.4 as a function of film thickness, following a master curve independent of spin speed and solvent. Drop cast films were found to follow a similar but distinct master curve.

NEXAFS. NEXAFS is an element-specific, bond-sensitive spectroscopy that can reveal orientation preferences for bond ensembles. Spectra are collected over an energy range within 30 eV of the K-shell ionization edge. Bound state transitions of K-shell electrons can occur both above and below the edge, and these transitions are differentiated by bond type. NEXAFS spectra of recrystallized films investigated in this study are shown in Figure 4. The lowest energy peak at 285.3 eV is the 1s → π^* transition of carbon double bonds within the thiophene units of the polymer backbone. The peak at 287.7 eV is a combination of carbon−hydrogen 1s → σ^* transitions, carbon−sulfur 1s → σ^* transitions, and Rydberg excitations. The ionization edge occurs at ≈290 eV; the spectra are normalized to an edge jump of unity by the intensity at 330 eV. The peaks above the edge jump are carbon−carbon 1s → σ^* transitions.

The greatest incident angular variation in the NEXAFS spectra is in the 1s → π^* transition that is oriented perpendicular to the ring plane. The orientation of this transition relative to the primary chemical structure of the HT-P3HT molecule is illustrated in Figure 5. In the HT-P3HT spectra shown in Figure 4a, the 1s → π^* resonance is greatest at near-normal incident angles, while least at glancing; this dependence indicates an edge-on orientation of the π plane. We quantify the degree of π plane orientation for all films investigated in this study using the figure of merit R described earlier, based on extrapolation of the angular variation of the 1s → π^* intensity as shown in Figure 4b. The results for R are compiled in Table 2. All as-cast films exhibit almost no preference in ring plane tilt ($R \approx 0$) regardless of side-chain length or regioregularity, although there is a slight preference for a face-on orientation ($R < 0$). After recrystallization, the R quantities become significantly more positive for the HT-P3ATs, indicating that the ring plane tilt distribution is biased toward an edge-on orientation. The ring planes of R-P3HT do not reorganize and remain essentially isotropic, consistent with the significant torsional disorder suggested by the UV−vis data.

Vibrational Spectroscopy. FTIR spectroscopy can discern structural information from individual moieties of the polymer as the vibrational resonances of different functional groups can be observed independently. This study focused on vibrational resonances from the polymer backbone and the alkyl side chains to independently monitor the changes of these portions of the molecule that occur upon recrystallization. The fingerprint region (1300−1600 cm^{-1}) contains features originating from backbone stretching modes (Figure 6). Caution is required when interpreting data in this region due to crowding of the spectra and the relatively weak IR signals observed from the thin films used in these experiments. This is especially true for the *s*-polarized data where the remnants of an etalon fringe, resulting from the IR transmission through the parallel Si wafer, further complicate the spectra.

There is a clearly resolved feature near 1510 cm^{-1} in both of the regioregular samples assigned to the fully anti-symmetric carbon−carbon stretches of the polymer backbone (ν_aC═C).[32] Previous work has demonstrated that the intensity and position of this feature are sensitive to the conjugation length along the thiophene backbone.[32] Importantly, this feature is absent in R-P3HT spectra. The position and dichroism of ν_aC═C, as determined from simultaneous fits to both *s*- and *p*-polarized

(26) Arwin, H.; Martensson, J.; Jansson, R. *Appl. Opt.* **1992**, *31* (31), 6707−6715.
(27) Arwin, H.; Jansson, R. *Electrochim. Acta* **1994**, *39* (2), 211−215.
(28) Jansson, R.; Arwin, H.; Gustafsson, G.; Inganas, O. *Synth. Met.* **1989**, *28* (1−2), 371−376.
(29) Zhokhavets, U.; Goldhahn, R.; Gobsch, G.; Schliefke, W. *Synth. Met.* **2003**, *138* (3), 491−495.
(30) Zhokhavets, U.; Gobsch, G.; Hoppe, H.; Sariciftci, N. S. *Thin Solid Films* **2004**, *451−52*, 69−73.
(31) Zhokhavets, U.; Gobsch, G.; Hoppe, H.; Sariciftci, N. S. *Synth. Met.* **2004**, *143* (1), 113−117.
(32) Hernandez, V.; Casado, J.; Ramirez, F. J.; Zotti, G.; Hotta, S.; Navarrete, J. T. L. *J. Chem. Phys.* **1996**, *104* (23), 9271−9282.

Table 2. Dichroism Figures of Merit for Thin P3AT Films Spun on HMDS Treated Substrates as Determined by UV−Vis, SE, FTIR, and NEXAFS

	SE $\epsilon_z/\epsilon_{x,y}$ at 2.25 eV[a]	NEXAFS R[b]	FTIR ν_a C=C A_p/A_s and (position)[c,d]	FTIR ν_s CH_2 A_p/A_s and (position)[c,d]	FTIR ν_a CH_2 A_p/A_s and (position)[c,d]
R-P3HT as-cast	0.60	−0.05	N/A	0.49 (2854.7 cm^{-1})	0.55 (2925.1 cm^{-1})
R-P3HT CM[e]	0.51	−0.04	N/A	0.46 (2854.9 cm^{-1})	0.51 (2926.5 cm^{-1})
HT-P3HT as-cast	0.12	−0.08	0.24 (1510.6 cm^{-1})	0.56 (2853.3 cm^{-1})	0.55 (2926.0 cm^{-1})
HT-P3HT CM[e]	0.11	0.29	0.19 (1510.0 cm^{-1})	0.47 (2854.8 cm^{-1})	0.51 (2925.9 cm^{-1})
HT-P3OT as-cast	0.11	−0.04	0.24 (1510.5 cm^{-1})	0.51 (2853.3 cm^{-1})	0.56 (2924.4 cm^{-1})
HT-P3OT CM[e]	0.08	0.34	0.24 (1509.6 cm^{-1})	0.41 (2853.7 cm^{-1})	0.47 (2924.1 cm^{-1})

[a] The standard deviation for the SE dichroism is ±0.08, based on the pooled variance of multiple spectra (two to three) for most samples. [b] The standard deviation for the NEXAFS R is ±0.01, based on the pooled variance of multiple spectra (two to three) for most samples. [c] The standard deviation for the FTIR dichroism is ±0.05, based on the pooled variance of multiple spectra (two to three) for most samples. [d] The standard deviation for the FTIR position is ±0.7 cm^{-1}, based on the pooled variance of multiple spectra (two to three) for most samples. [d] CM: crystallized from the melt.

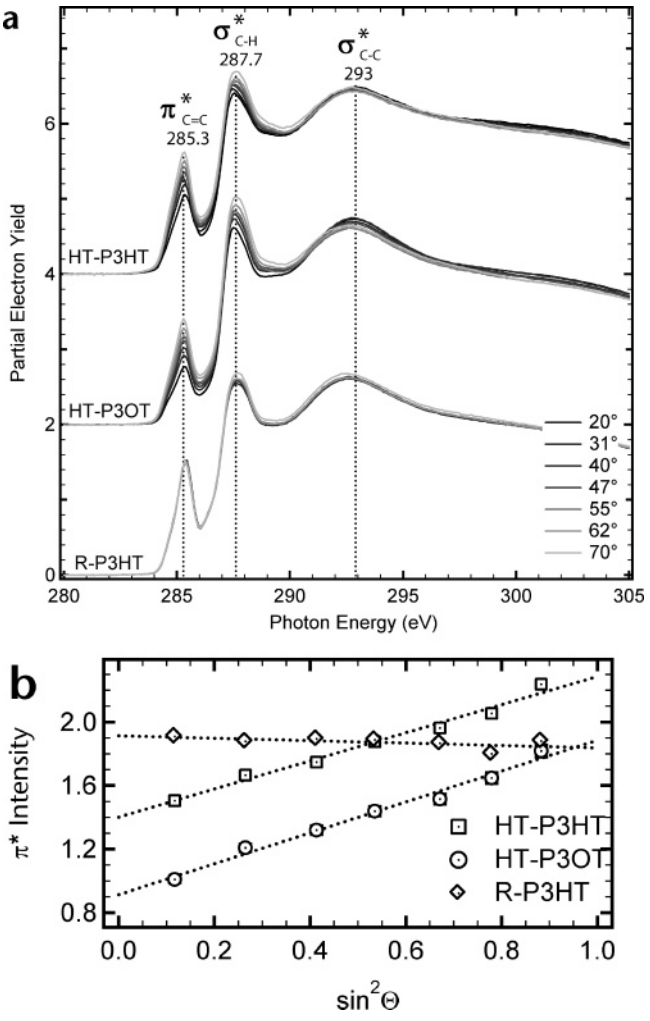

Figure 4. (a) Angle-dependent NEXAFS spectra of HT-P3HT, HT-P3OT, and R-P3HT films after recrystallization. (b) Variation of 1s → π^* transition intensity with squared sine of incident angle Θ for spectra shown in panel a.

data, are reported in Table 2. The position for HT-P3HT and HT-P3OT is consistent with a conjugation length in excess of five thiophene units, based on the reported position of the mode in thiophene oligomers.[33]

The vibrational features in the 2800−3000 cm^{-1} region of the spectra, Figure 7, relate to the CH stretches of the alkyl side chains with a weak feature at 3050 cm^{-1} assigned to an aromatic

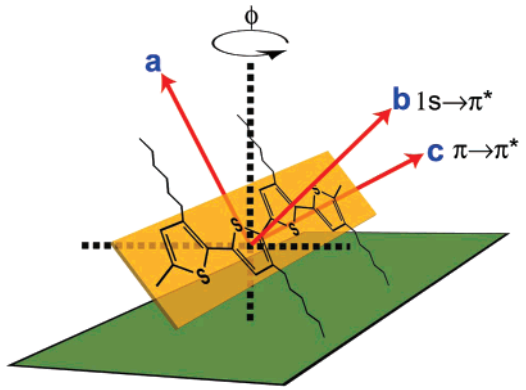

Figure 5. Definition of polymer-chain frame (a−c) and orientation angles (θ, ψ, ϕ) for P3AT. The labeling a−c follows that of the conventional unit cell for crystallites. The s → π^* transition in NEXAFS is along the *b* axis, and the π → π^* transition in SE is along the *c* axis.

CH stretch. The largest peak in this region is the anti-symmetric stretch of the methylene units ($\nu_a CH_2$, ≈2925 cm^{-1}). The $\nu_a CH_2$ frequency is known to be sensitive to conformation and typically appears near 2918 cm^{-1} in crystalline, all-trans environments and near 2928 cm^{-1} in disordered, liquid-like environments.[34,35] The frequencies observed for HT-P3HT (Table 2) are indicative of significant disorder, independent of the thermal history. The $\nu_a CH_2$ frequencies for HT-P3OT are slightly red-shifted from those of HT-P3HT, indicating more trans order in the chains. Yet, like P3HT, the $\nu_a CH_2$ frequency does not change significantly upon heating. Similar to the CH_2 frequencies, the dichroism values (Table 2) do not change significantly upon thermal treatment for any of the films. Also reported in Table 2 are the observed ν and dichroism values for the $\nu_s CH_2$ symmetric stretch. The dichroism values are essentially the same as for $\nu_a CH_2$. Like $\nu_a CH_2$, neither $\nu_s CH_2$ nor its dichroism change significantly upon thermal treatment.

Discussion

Even though a dynamic range of $>10^4$ is spanned by the wavelengths involved: ≈10 μm for IR transmission and ≈4.0

(33) Hernandez, V.; Casado, J.; Ramirez, F. J.; Zotti, G.; Hotta, S.; Navarrete, J. T. L. *Synth. Met.* **1996**, *76* (1−3), 277−280.
(34) Snyder, R. G.; Maroncelli, M.; Strauss, H. L.; Hallmark, V. M. *J. Phys. Chem.* **1986**, *90* (22), 5623−5630.
(35) Snyder, R. G.; Strauss, H. L.; Elliger, C. A. *J. Phys. Chem.* **1982**, *86* (26), 5145−5150.

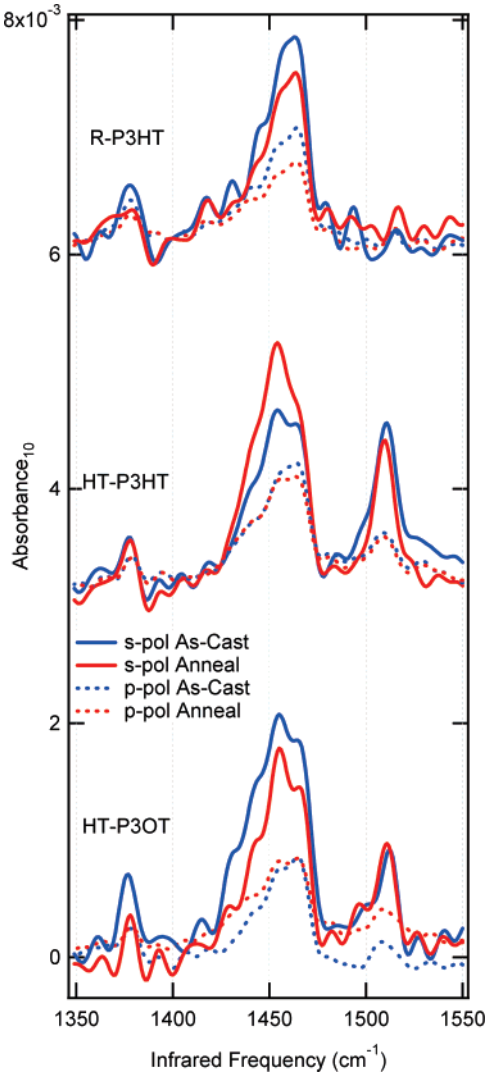

Figure 6. FTIR spectra of P3AT films on HMDS treated silicon wafers before (blue) and after (red) heating. Spectra were taken with *s*-polarized (solid line) and *p*-polarized (dashed line) light while the substrate was held at Brewster's angle with respect to the incoming IR beam. Data from the different polymers have been offset for clarity.

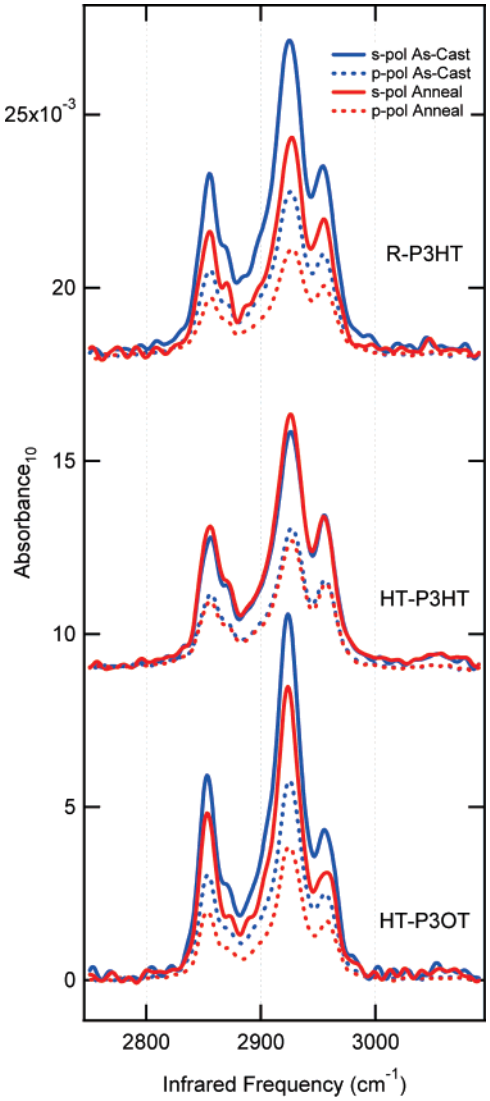

Figure 7. FTIR spectra of P3AT films on HMDS treated silicon wafers before (blue) and after (red) heating. Spectra were taken with *s*-polarized (solid line) and *p*-polarized (dashed line) light while the substrate was held at Brewster's angle with respect to the incoming IR beam. Data from the different polymers have been offset for clarity.

nm for NEXAFS, the data for the optical techniques can be uniformly treated in the context of the dielectric constant tensor ϵ for the film. For each spectroscopy, ϵ will be developed, consistent with the transition dipole moment for the dominant transitions: the $\pi \rightarrow \pi^*$ in the visible region, the s $\rightarrow \pi^*$ in the X-ray region, and the dipole active vibrational transitions of the polymer backbones ($\nu_a C{=}C$) and side chains ($\nu_a CH_2$). Assuming in-plane isotropy (consistent with both SE and NEXAFS failures to observe significant in-plane anisotropy), ϵ will be diagonal, with only two distinct elements: ϵ_z and $\epsilon_{x,y}$. ϵ can be expressed in terms of an average of the dielectric tensor in the frame of reference of the polymer chain (*a*, *b*, *c*), over an orientation distribution, *f*, given by the Euler angles θ, ψ, and ϕ (see Figure 5), and the distribution in ϕ is assumed isotropic. For each spectroscopy, we will chose the polymer frame of reference (*a*, *b*, *c*) such that the transition dipole is along *c*. For this choice, ϵ becomes a function of $\langle \cos \theta^2 \rangle$.

One of the most important orientation quantities of any semiconducting organic molecule is the tilt of its conjugated plane with respect to the film plane. Increased vertical (edge-on) orientation of this conjugated plane will allow increased $\pi{-}\pi$ overlap between molecules in the plane of the conduction channel and presumably enhance intermolecular carrier transport.[13,14] NEXAFS is the most straightforward spectroscopy for analysis, as, in the X-ray region, local field effects (Snell's law) can be neglected. Therefore, the signal can then be directly interpreted as the dot product of the incident electric field vector **E** and the transition dipole moment for the 1s $\rightarrow \pi^*$ transition, which lies perpendicular to the ring plane (see Figure 5), where **E** is given directly from the angle of incidence Θ. Allowing for nonidealities in the polarization state of the X-ray beam (fraction *p*-polarized *P*), the NEXAFS signal can be expressed as

$$\text{signal} \sim \frac{1}{2}\left(1 - \langle \cos 2\theta \rangle + \frac{1}{2}(1 + 3(2\langle \cos^2 \theta \rangle - 1)P\cos^2 \theta)\right) \quad (1)$$

where θ is the tilt of the transition dipole vector from the surface normal, $\langle\ \rangle$ is an average over the orientation distribution, *f*, and

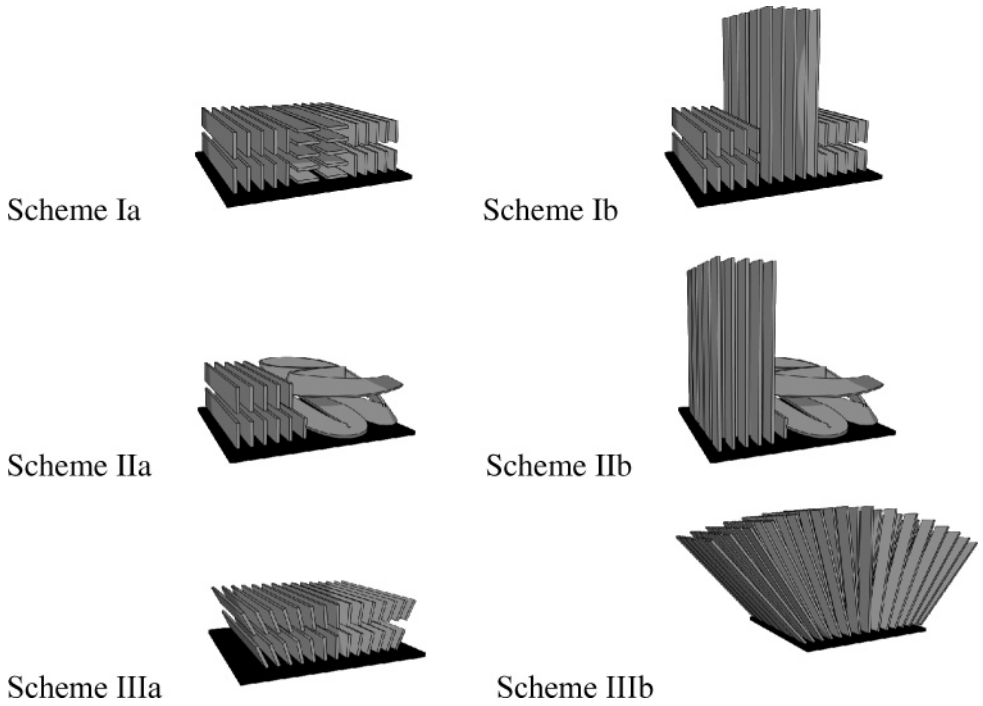

Figure 8. Schematic of possible trial orientational distributions of P3AT molecules when cast into thin films. Schemes a are appropriate to the discussion of NEXAFS (that determines the polymer-chain *b* axis alignment), while schemes b are appropriate to the discussion of SE (that determines the polymer-chain *c* axis alignment).

θ is the angle of incidence of the X-ray beam from the surface plane. The figure of merit, *R*, becomes

$$R = \frac{I(90°) - I(0°)}{I(90°) + I(0°)} = \frac{P(1 - 3\langle\cos^2\theta\rangle)}{2(1 - \langle\cos^2\theta\rangle) + P(3\langle\cos^2\theta\rangle - 1)} \quad (2)$$

where *I* is the measured intensity. Ideally, the figure of merit *R* would be −1 for pure face-on order and 1 for pure edge-on order; however, due to $P \approx 0.85$, the limiting value for edge-on order is found to be 0.7. For an isotropic distribution ($\langle\cos^2\theta\rangle = 1/3$), *R* is 0. Because linear techniques only measure one moment of the orientation distribution, it is necessary to assume a trial distribution to visualize a given $\langle\cos^2\theta\rangle$. Shown in Figure 8 are pictorial representations of possible trial distributions (*f*) for the polymer chains. Because of the semicrystalline nature of the polymer, we focus on distributions that contain crystalline regions. In Scheme 1a, all of the film is assumed to be crystalline, with the crystallites adopting either edge-on or face-on order. In Scheme 2a, the film is a mixture of edge-on crystallites and amorphous ($R = 0$) regions, while in Scheme 3a, the film is assumed to be uniform, with a broad distribution about the edge-on orientation. Other schemes can be adopted.

The near zero *R* observed for all as-cast films suggests either a 50−50 mix of orthogonally oriented crystallites (Scheme 1a) or an isotropic distribution (Scheme 3a). An isotropic distribution is consistent with XRD[10] and GIXD[9] of similarly prepared, high MW films, in which no significant diffraction is observed. The high value of *R* (≈0.3) observed for the recrystallized films is remarkable. Assuming Scheme 1a, an upper limit on the edge-on fraction of ≈80% is obtained. Assuming the more realistic Scheme 2a, still 45% of the film is edge-on crystallites. Within Scheme 3a, $R \approx 0.34$ implies a top-hat distribution of angles of nominally 45° half-width about the ideal edge-on orientation. For a narrow distribution about a single angle, $R \approx 0.29-0.34$ implies $\theta \approx 64-66°$.

It is notable that the single feature in the UV−vis spectroscopy that best correlates to the development of high order in the π system director is the development of the exciton−polaron fine structure. In a recent charge modulation spectroscopy study, this fine structure was resolved into two components:[15] a single feature at 2.03 eV attributed to an interchain exciton and a Franck−Condon series at 2.27 eV attributed to the intrachain excition−polaron. Our data are equally consistent with a single Franck−Condon series with an origin at 2.03 eV or two series. The strong correlation between the structure at 2.03 eV with the NEXAFS evidence for significant order in the chain π director is equally consistent with a stronger intrachain vibronic coupling, due to improved planarity of the chain, or a stronger interchain exciton, due to improved chain−chain packing.

The transition dipole moment for the $\pi-\pi^*$ transition observed in SE lies along the main-chain axis (*c*).[25] Within a linear effective medium approximation, the dielectric function for the film can be expressed in terms of the dielectric function in the frame of the polymer chains as

$$\epsilon = \begin{pmatrix} \epsilon_{xy} & 0 & 0 \\ 0 & \epsilon_{xy} & 0 \\ 0 & 0 & \epsilon_z \end{pmatrix} = \mathbf{R}^{-1}(\theta) \begin{pmatrix} \epsilon_{ab}' & 0 & 0 \\ 0 & \epsilon_{ab}' & 0 \\ 0 & 0 & \epsilon_c' + i\epsilon''_c \end{pmatrix} \mathbf{R}(\theta) \quad (3)$$

where **R** is a rotation matrix from the *abc* frame to the *xyz* frame (as a function of the tilt of the *c* axis from the surface normal θ, averaged over the twist ψ and twirl ϕ Euler angles), and absorption is only along the chain axis *c* direction. It can be shown that the ratio of the imaginary parts of the film dielectric function can be expressed as

$$\frac{\epsilon''_z}{\epsilon''_{xy}} = 2\frac{\langle\cos^2\theta\rangle}{\langle\sin^2\theta\rangle} \quad (4)$$

This result is essentially equivalent to that of McBranch et al.[36] More sophisticated effective medium models have been developed

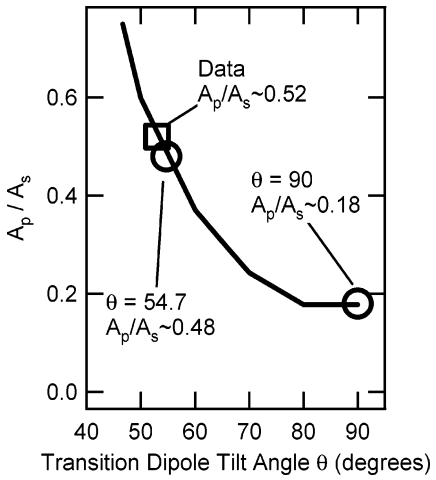

Figure 9. Plot of a simulation of the FTIR figure of merit (A_p/A_s), assuming a film of 25 nm thickness, with $\epsilon_{ab} = 2.40$, ϵ_c given by eq 5, and f given by a delta function distribution in θ, the transition dipole tilt angle from the surface normal.

for anisotropic inclusions in isotropic matrixes.[37] Numerical studies suggest that they represent less than a 10% correction to the simple model for ϵ representative of the systems studied here.

On the basis of results in Table 2, the level of chain axis, *c*, order for the HT films is quite significant. If Scheme 1b is assumed (appropriate trial distributions for *c* axis order have the crystallites either side-on or head-on), approximately >95% of the film has *c* in the plane of the surface. Additionally, Scheme 1b would predict (in the linear effective medium approximation) that the ϵ''_z spectrum be identical to that of $\epsilon''_{x,y}$. That is not supported by the data. There is a consistent blue-shift in the absorption maximum for ϵ''_z, and the fine structure is less prominent. This data suggests that Scheme 2b (side-on chains and amorphous regions) is more appropriate and that the ϵ''_z absorption arises from disordered regions of the film with shorter conjugation length. Within Scheme 2b, the observed dichroism implies that 85% of the film has the *c* axis in the surface plane. The observation that the SE anisotropy in the films does not significantly change upon crystallization from the melt may indicate that the ϵ''_z absorption arises from hairpin or other fold structures that are kinetically locked, even above the melting point. If we presume a Scheme 3b distribution, the anisotropy in ϵ is consistent with a top-hat spread in θ of $\pm 22°$ about 90°.

Unlike with the SE, the polarized IR data do not support a unique determination of the relevant dielectric tensor ϵ. However, the figure of merit A_p/A_s can be forward simulated based on trial orientation distribution functions and the assumption of an ϵ given by eq 3. This approach is similar in spirit to that of Harder et al.[38] Shown in Figure 9 is a graph of the forward simulated A_p/A_s, assuming a film of 25 nm thickness, with $\epsilon_{ab} = 2.40$, $\epsilon_c = (2.40 + A\Gamma\upsilon_o)/(\upsilon^2 - \upsilon_o^2 - I\Gamma\upsilon)$, and f given by a delta function distribution in θ. For a transition dipole directed entirely along the surface normal ($\theta = 0$), the figure of merit diverges; for one directed entirely in the plane of the surface, the figure of merit is ≈0.18, while for an isotropic distribution (in the Scheme 3 sense) $A_p/A_s \approx 0.48$. The forward simulation is sensitive to the choice of the ϵ' offset. The choice $\epsilon_{ab'} = 2.40$ ($n_{ab} = 1.55$) was based on $\epsilon_{xy'} = 2.40$ determined from IR ellipsometry measurements near 2900 cm^{-1}. The in-plane index of refraction for these films is high in the near-IR [n_{xy}(1000 nm) ~ 1.69], due to dispersion arising from the strong visible absorption. However, in the mid-IR, one is sufficiently removed from the strong electronic transitions that an index in the range 1.55−1.45 is expected, consistent with the IR ellipsometry measurement.

The long axis orientation for HT-P3HT and HT-P3OT was confirmed by the IR dichroism of the ν_aC═C resonance. This feature, prominent in the HT-P3HT and HT-P3OT spectra at 1510 cm^{-1} (Figure 6), fails to clearly rise above the noise in the R-P3HT sample. As with the visible dichroism ($\epsilon''_z/\epsilon''_{x,y}$), the dichroism figure of merit for the infrared data (A_p/A_s) indicates that the polymer's long-chain axis lies within the plane of the film and is unaffected by recrystallization for the regioregular polymers. However, the increased disorder in the regiorandom polymer's backbone appears to attenuate intensity from this feature in the spectra. On the basis of Figure 9, the A_p/A_s of the ν_aC═C of 0.24−0.19 suggest that $\langle\cos\theta^2\rangle$ lies in the range of 0.11−0.05, consistent with the range of 0.06−0.04 given by eq 4 and the SE $\epsilon''_z/\epsilon''_{x,y}$.

The precise structure of the alkyl chains in crystalline regions of P3ATs is not clearly established. The lamellar spacing observed in X-ray diffraction is inconsistent with noninterdigitating, all-trans side chains in the backbone plane.[39,44] Either the alkyl-chains interdigitate or some combination of tilt of the intermolecular plane and twist of the alkyl chain out of the plane of the backbone is required to achieve the compact lamella spacing. X-ray diffraction studies on stretch oriented films[39,44] have generally been interpreted in terms of tilted, nearly all-trans chains, although an interdigitated polymorph has been reported.[40] Our present polarized IR data are incompatible with all-trans, interdigitated chains in the plane of the backbone. The $\nu_a CH_2$ transition moment distribution function would then be identical to 1s → π*, and A_p/A_s should be ≈0.3. Similarly, we can exclude a rigid tilt of the entire chain plane.[40] Assuming an all-trans chain, the dichroism values in Table 2, combined with Figure 9, allow us to determine the tilt θ and twist ψ of the side-chain long axis. For recrystallized HT-P3HT and HT-P3OT films, the results are $\theta = 56°$, $\psi = 46°$, $\theta = 52°$, and $\psi = 47°$, respectively. Nearly identical chain orientations are derived for the other films in Table 2. The six conditions in Table 2 pooled are consistent with $\theta = 57 \pm 4°$ and $\psi = 46.3 \pm 0.6°$. The chain tilt is essentially the magic angle, 54.7°, expected for an isotropic or disordered system. The near liquid-like $\nu_a CH_2$ frequencies observed for HT-P3HT are additionally indicative of disorder. The $\nu_a CH_2$ frequencies for HT-P3OT do suggest slightly more trans order in the chains, but the chains are still far from the high degree of order characteristic of high density alkane monolayers. The IR results clearly indicate that the side chains are in a disordered, liquid-like state for all films prepared. This conclusion is supported by the strong similarity between the HT-P3HT and the R-P3HT IR spectra, as the chains in the R-P3HT are expected to lack significant order. Significantly disordered side chains are consistent with their low density. On the basis of the reported crystallite repeat dimensions, ≈0.78 nm in both the *a* and *b*

(36) McBranch, D.; Campbell, I. H.; Smith, D. L.; Ferraris, J. P. *Appl. Phys. Lett.* **1995**, *66* (10), 1175−1177.
(37) Levy, O.; Stroud, D. *Phys. Rev. B* **1997**, *56* (13), 8035−8046.
(38) Harder, P.; Bierbaum, K.; Woell, C.; Grunze, M.; Heid, S.; Effenberger, F. *Langmuir* **1997**, *13* (3), 445−454.
(39) Tashiro, K.; Kobayashi, M.; Kawai, T.; Yoshino, K. *Polymer* **1997**, *38* (12), 2867−2879.
(40) Prosa, T. J.; Winokur, M. J.; McCullough, R. D. *Macromolecules* **1996**, *29* (10), 3654−3656.
(41) Onclin, S.; Ravoo, B. J.; Reinhoudt, D. N. *Angew. Chem., Intl. Ed.* **2005**, *44* (39), 6282−6304.
(42) Kline, R. J.; McGehee, M. D.; Kadnikova, E. N.; Liu, J. S.; Frechet, J. M. J. *Adv. Mater.* **2003**, *15* (18), 1519.
(43) Wang, G. M.; Hirasa, T.; Moses, D.; Heeger, A. J. *Synth. Met.* **2004**, *146* (2), 127−132.
(44) Prosa, T. J.; Winokur, M. J.; Moulton, J.; Smith, P.; Heeger, A. J. *Macromolecules* **1992**, *25*, 4364−4372.

directions, the areal density of side chains in a crystalline lamella is only 3.3×10^{14} cm^{-2}, to be compared with $>4.5 \times 10^{14}$ cm^{-2} in dense, well-ordered alkane self-assembled monolayers.[41] Similarly, if we estimate the volume density between the lamella, allowing for an excluded layer of ~0.35 nm for the backbone, we arrive at a liquid-like 0.7 g/cm^3.[45]

The combined data of the three spectroscopies clearly suggest that the as-cast HT films have high *c* order but are disordered in *b*. Recrystallization significantly improves the *b* order, as reflected in both the NEXAFS and the development of well-resolved exciton−polaron structure in the UV−vis. It is remarkable that, despite the significant changes in *b* order upon recrystallization, the CH_2 transition dipoles of the alkyl chains exhibit dichroism consistent with an isotropic distribution that does not change upon recrystallization. This observation strongly suggests that the ordering of the backbone is not driven by the development of van der Waals order in the alkyl side chains but, instead, that the side chains have adequate conformational flexibility to not interfere with the backbone ordering. The lamella observed in X-ray diffraction[10,24,42] appear to be separated by significantly disordered side chains.

Using the clarity of the exciton−polaron features in the UV−vis as a simple diagnostic for backbone order, we find that the bulk of the films characterized in the literature is nominally consistent with our as-cast films and thus have significant structural disorder. The recrystallized P3OT films of Sakurai et al. have very pronounced fine structure.[23] Unfortunately, no transport measurements were reported for those films. Dip-cast HT-P3HT films reported by Wang et al. also have a pronounced fine structure and result in mobilities of ≈0.2 cm/V s.[43] This suggests that the high level of structural order achieved by recrystallization should result in improved electrical performance. As the ring-plane tilt order parameters for HT-P3OT are in general similar to, if not superior to, those of HT-P3HT, it also suggests that detailed transport studies of that polymer could be informative. We note in passing that heating polyalkylthiphenes above the melting point is occasionally problematic. In preliminary studies of low molecular weight (<10 kDa) HT-P3HT films, dewetting occurred at elevated temperatures. Similarly, dewetting occurs when higher molecular weight films are melted on high water contact angle substrates, such as those created by octadecyltrichlorosilane functionalization.

(45) For HT-P3HT, the reported two chain cell dimensions are $a = 1.67$ nm, $b = 0.78$ nm, and $c = 0.78$ nm. Assuming 24 CH_2 in the (1.67−0.35)(0.78)(0.78) nm^3 volume results in $\rho = 0.69$ g/cm^3.

Conclusion

A suite of optical measurements was employed to characterize the structure of as-cast and crystallized from the melt R-P3HT, HT-P3HT, and HT-P3OT films. The data for the optical techniques can be uniformly treated in the context of the dielectric constant tensor ϵ for the film to provide a consistent description of the molecular order. Both heating above the melting point and extensive recystallization just below is required for the development of maximum order. The polymer-chain long axis is highly ordered in both as-cast and crystallized from the melt films. The conjugated plane π orbital director, thought to be a sensitive diagnostic for the development of 2-D band structure and high mobility, is disordered in as-cast films but significantly ordered after crystallization from the melt. The variation in the π order directly correlates with the Franck−Condon fine structure in the visible absorption spectrum. The extensive ordering of the backbone appears uncorrelated with the akyl chains, which exhibit significant disorder even after crystallization from the melt for all preparation conditions.

Acknowledgment. The authors thank Ganesh Ramachandran, James Batteas, and Caroline Kitchens for preliminary AFM studies as well as Edwin Heilweil for use of the UV−vis spectrometer. M.G. and B.M.V. are supported by a NIST/NRC fellowship.

LA0618972